Leaf excision has minimal impact on photosynthetic parameters across crop functional types

John N. Ferguson[1,2*], Tamanna Jithesh[1†*], Tracy Lawson[2] and Johannes Kromdijk[1,3]
[1]Department of Plant Sciences, University of Cambridge, Cambridge, Cambridgeshire, CB2 3EA, UK
[2]School of Life Sciences, University of Essex, Wivenhoe Park, Colchester, Essex CO4 3SQ, UK
[3]Institute for Genomic Biology, University of Illinois at Urbana-Champaign, Urbana, Illinois, 61801, USA
[†]Current address: Centre for Crop and Environmental Science, Harper Adams University, Edgmond, Shropshire TF10 8NB, UK
[*]Equal contribution

Highlight

Across the main photosynthesis functional types (C_3-dicot, C_3-monot, and C_4-monot) of major crops (tomato, barley, and maize), measurements of photosynthetic parameters demonstrate few, but important, differences when measured on excised relative to intact leaves.

Abstract

Photosynthesis is increasingly becoming a recognised target for crop improvement. Phenotyping photosynthesis-related traits on field-grown material is a key bottleneck to progress here due to logistical barriers and short measurement days. Many studies attempt to overcome these challenges by phenotyping excised leaf material in the laboratory. To date there are no demonstrated examples of the representative nature of photosynthesis measurements performed on excised leaves relative to intact leaves in crops. Here, we tested whether standardised leaf excision on the day prior to phenotyping impacted a range of common photosynthesis-related traits across crop functional types using tomato (C3-dicot), barley (C3-monocot), and maize (C4-monocot). Potentially constraining aspects of leaf physiology that could be forecasted to impair photosynthesis in excised leaves, namely leaf water potential and abscisic acid accumulation, were not different between intact and excised leaves. We also observed non-significant differences in spectral reflectance and chlorophyll fluorescence traits between the treatments across the three species. However, we did observe some significant differences between gas exchange and photosynthetic capacity associated traits across all three species. This study represents a useful reference for those who perform measurements of this nature and the differences reported should be considered in associated experimental design and statistical analyses.

Keywords

Leaf excision, photosynthesis, leaf reflectance, chlorophyll fluorescence, *Solanum lycopersicum*, *Hordeum vulgare*, *Zea mays*

Abbreviations

ABA	Abscisic acid
A_N	Net photosynthetic CO_2 assimilation
c_i	Intracellular CO_2 concentration
F_m	Dark adapted maximum fluorescence
F_m'	Maximum fluorescence
F_v/F_m	Maximum photosystem II efficiency
g_s	Stomatal conductance
iWUE	Intrinsic water use efficiency
J_{max}	Maximum rate of electron transport for RuBP regeneration
LWI	Leaf Water Index
MSI	Moisture Stress Index
NDNI	Normalised Difference Nitrogen Index
NPQ	Non-photochemical quenching
PAR	Photosynthetically active radiation
RE-NDVI	Red Edge-Normalised Difference Vegetation Index
V_{cmax}	Maximum rate of Rubisco carboxylation
V_{pmax}	Maximum rate of PEPc carboxylation
V_{max}	Maximum rate of photosynthesis

Introduction

The global demand for food is expected to double by the middle of this century. Human population growth means that the rate of increase in food demand outpaces the annual rate of increase in crop productivity (Zhu *et al.*, 2010; Kromdijk and Long, 2016; Lenaerts *et al.*, 2019). This mismatch highlights the necessity to adopt novel crop improvement targets to achieve food security (Gojon *et al.*, 2023). As the primary determinant of biomass accumulation, photosynthesis represents a sensible target to this end. Evidence from free air CO_2 enrichment experiments has highlighted how increasing CO_2 assimilation can lead to improved crop yields (Ainsworth and Long, 2021). Similarly, transgenic improvements to independent aspects of photosynthetic biochemistry have demonstrated that increasing carbon fixation is a realistic strategy for increasing yield (Driever *et al.*, 2017; Yoon *et al.*, 2020; De Souza *et al.*, 2022).

Targeting photosynthesis in crop improvement efforts necessitates the ability to screen many hundreds or thousands of genotypes for photosynthesis-associated traits. This is important for quantifying variation to incorporate in selection models. Additionally, it is necessary for facilitating forward genetics to identify novel genes or genetic regions underlying said variation to target through molecular approaches, such as marker-assisted breeding or direct manipulation through genome editing. This is challenging because the gold-standard methods through which many photosynthesis-associated traits are phenotyped are often logistically challenging to perform in field trial-like environments and they are time consuming (Long, 2003; Walker *et al.*, 2018). Standard methodologies, such as the commonly performed photosynthesis-CO_2 response (A-c_i) measurement used for modelling photosynthetic capacity can take up to 45-60 minutes to perform per sample. This is problematic because it limits the number of measurements that can be performed per day. This is especially true in the field relative to controlled conditions, where diurnal weather effects on physiological patterns, such as decreasing leaf water potential, photosystem II efficiency, and chloroplastic inorganic phosphate concentration, can transiently impact photosynthetic activity and the length of the measurement day (Murchie *et al.*, 1999; Leakey *et al.*, 2006). Logistical challenges arise, for example, due to specialised equipment not being suitable for use within crop canopies and because of the lack of access to power supplies.

A potential means through which to overcome some of these confounding effects and logistical challenges is to excise leaf material from plants of interest and phenotype those leaves in a more amenable and stable laboratory setting. Studies on woody species have shown that phenotyping photosynthetic- and reflectance-associated traits on the leaves of excised branches generates data that is highly comparable to that generated through phenotyping leaves on branches still attached to the tree (Richardson and Berlyn, 2002; Miyazawa *et al.*, 2011; Akalusi *et al.*, 2021). Over the past decade, a similar approach has routinely been employed for multiple crop species (e.g., Driever *et al.*, 2014; Ferguson *et al.*, 2021; Montes *et al.*, 2022). Here, leaves, or tillers harbouring a leaf of interest, are excised from plants and the cut end is placed into water in an attempt to maintain hydraulic conductivity. For photo-physiological phenotyping, the maintenance of hydraulic efficiency is important for replacing water lost via transpiration (Müllers *et al.*, 2022), which is instrumental to keep stomata open for CO_2 uptake. It is possible that the demonstrable success of employing this approach with woody species is at least in part due to the presence of secondary xylem. Secondary xylem facilitates water transport, but it is also critical in protecting the primary xylem from mechanical damage (Miodek *et al.*, 2021), such as that that might ensue after branch excision. This presence of secondary xylem is a key anatomical difference that distinguishes the tree species where this approach has been demonstrated to work as effectively as *in-situ* phenotyping and the herbaceous annual crop species for which this technique is now regularly employed. Due to this key difference and others, it is plausible that the mechanistic basis that underpins the success of performing photosynthesis measurements on foliage of detached branches of woody species does not necessarily translate to herbaceous species. Consequently, a key knowledge gap exists here with respect to understanding the extent to which measurements made on excised leaves are representative of those made on intact leaves for crop species.

Addressing the above-described knowledge gap is a high-priority due to the rapid uptake of this approach for phenotyping photosynthesis in crop species. Variations on this technique have been reported in studies involving many key crop species, however we are not aware of any studies that employ this approach and show that the data they obtain are representative of what would have been obtained from intact material. Information to this end will be key for emphasising the value of this approach. Maize is perhaps the species with which this

122 approach has been most employed. For example, Markelz *et al.*, (2011) excised leaves from
123 maize plants growing in a free air CO_2 enrichment (FACE) experiment and under variable soil
124 nitrogen availabilities to perform A-c_i response measurements to test interactive effects of
125 CO_2 and nitrogen supply on photosynthetic capacity. Similarly, Liao *et al.*, (2022) phenotyped
126 excised maize leaves from plants growing under full- and deficit-irrigation to again perform
127 A-c_i response measurements to test how water availability influenced photosynthetic
128 capacity and stomatal limitations to photosynthesis. As well as phenotyping small numbers
129 of maize genotypes to test environmental interactions (See also: Leakey *et al.*, 2006) and
130 Choquette *et al.*, (2019)), this approach has also been employed for maize to facilitate
131 screening of large populations for forward genetics purposes. For example, Xie *et al.*, (2021)
132 used this approach to phenotype a mapping population consisting of 197 recombinant inbred
133 lines (RILs) for light-saturated gas exchange. By utilising this approach, this study was able to
134 identify genetic regions underpinning variation in photosynthesis and associated traits. An
135 identical approach has also been utilised for phenotyping genetic diversity in sorghum. Here,
136 this approach enabled by-far the largest survey of genetic variation in photosynthesis, where
137 over 800 genetically distinct sorghum varieties were characterised enabling genome- and
138 transcriptome-wide association mapping (GWAS and TWAS) to pinpoint precise genes
139 underlying variation in photosynthesis (Ferguson *et al.*, 2021). Phenotyping photosynthesis of
140 excised leaves has also been used in other C_4 species, such as Miscanthus, where this
141 approach has facilitated testing of the adaptation of photosynthesis to self-shading (Collison
142 *et al.*, 2020), and sugarcane, where it has facilitated testing of the response of photosynthesis
143 to the application of sugars (McCormick *et al.*, 2008).
144
145 Despite C_4 crops typically having more physiologically robust leaves, measuring
146 photosynthesis in excised material has also been performed on studies focusing on monocot
147 and dicot C_3 crops. For example, excised tillers were used to phenotype flag-leaves for a suite
148 of photosynthesis-related traits in a diversity set of 64 wheat accessions at different
149 developmental stages (Driever *et al.*, 2014; Carmo-Silva *et al.*, 2017). This approach has also
150 been used in barley where the leaf of interest was directly excised at its base rather than
151 harvesting the entire tiller to test how direct nitrate feeding impacted photosynthesis and
152 sugar synthesis (Morcuende *et al.*, 2005). In rice, excised leaf material has also been used to
153 measure chlorophyll fluorescence across distinct varieties to facilitate GWAS of fluorescence

154 parameters (Ferguson *et al.*, 2020). Similar fluorescence experiments on excised leaf
155 segments of wheat provided some preliminary evidence for an impact of the time between
156 excision and measurement, where a minimal waiting time may be needed to properly relate
157 observations to differences in photosynthetic efficiency (McAusland *et al.*, 2019). To the best
158 of our knowledge, utilisation of excised leaf material in C_3 dicots is constrained to studies on
159 soybean. For example, Morgan *et al.*, (2004) cut petioles of fully expanded leaves of soybean
160 plants growing in an open-air elevated ozone experiment to perform chlorophyll
161 fluorescence, A-c_i and photosynthesis light-response (AQ) measurements to understand the
162 photosynthetic response to ozone stress. The same technique was operated by Montes *et al.*,
163 (2022) to perform A-c_i measurements and concurrent measurements of hyperspectral
164 reflectance to build models for predicting photosynthetic capacity in the field and for
165 facilitating GWAS.
166
167 Excision plausibly elicits an abscisic acid (ABA) biosynthesis response in leaves in a manner
168 similar to that which promotes the stabilisation of leaf water status (Beardsell and Cohen,
169 1975) and/or resistance to herbivory (Vos *et al.*, 2013, 2019; Nguyen *et al.*, 2016). This is an
170 important consideration here since ABA accumulation within leaves also serves to close
171 stomatal apertures and reduce transpirational water loss in response to drought, which
172 consequently impairs carbon uptake (Blatt, 2000; Schroeder *et al.*, 2001). Further to this,
173 there may well be a myriad of minor-to-major alterations of leaf properties, e.g., changes to
174 xylem tension, cell turgor, leaf water potential, pigmentation, etc. (Govindjee *et al.*, 1981;
175 Carter, 1991; Canny, 1997; Richardson and Berlyn, 2002; Tyree and Cochard, 2003), that could
176 impact the photosynthetic activity of excised leaves. Due to the reality of these potential
177 pitfalls and because of our reliance on performing photosynthesis measurements on excised
178 leaf material in crop research, it is critical to understand whether leaf excision impacts
179 photosynthesis in crop species. To this end and with this study we tested how standardised
180 leaf excision on the day before phenotyping impacted light-saturated photosynthesis,
181 photosynthetic capacity, chlorophyll fluorescence, hyperspectral reflectance, ABA
182 accumulation and leaf water potential. For this we employed reference genotypes of tomato,
183 barley, and maize, which represent the main photosynthesis functional types of crops, i.e., C_3
184 monocot, C_3 dicot and C_4 monocot.
185

186 # Materials and methods

187 ## Plant Material and Experimental Design

188 Reference genotypes for tomato, barley and maize were used for this study. These genotypes
189 were M83 (tomato), Golden Promise (barley), and B73 (maize). All plants were grown at the
190 Plant Growth Facility of the University of Cambridge. Seeds from all species were sown into
191 modular trays before being transplanted into larger pots once the seedlings were established.
192 Barley and tomato were grown in 1.5L sized pots. Maize was grown in 6L sized pots with two
193 plants per plot. Barley was grown in multipurpose compost (M3 Compost, Levington Ltd., UK).
194 Tomato was grown in a seedling and cuttings compost (F2 Compost, Levington Ltd., UK) and
195 fertilised with specialised tomato feed (Tomorite, Levington Ltd., UK). Maize was grown in a
196 2:1 mix of these two compost types with added perlite. Tomato and maize were grown in the
197 same growth room where the photoperiod was set to 14 hours. The light level was set to 600
198 µmol m^{-2} s^{-1} photosynthetically active radiation (PAR). The humidity was set to 65% relative
199 humidity (RH). The air temperature was set to 28°C in the daytime and 20°C in the night-time.
200 The growth room of the barley was set to a 16-hour photoperiod. The light level was set to
201 400 µmol m^{-2} s^{-1} PAR. The humidity was set to 60% RH. The air temperature was set to 22°C
202 in the daytime and night-time.
203
204 Prior to any given measurement day, plants were transferred from the Plant Growth Facility
205 to the laboratory at the Department of Plant Sciences (University of Cambridge) at 14.00 h.
206 All plants were checked to be well watered and left on the laboratory bench. At 17.00 h, those
207 plants that were to be measured as excised were cut. For tomato, the youngest fully expanded
208 leaf was cut at the petiole below the two leaflets adjacent to the terminal leaflet. The petiole
209 was then immediately placed under water and recut before being transferred to a 15 ml
210 falcon tube under water. For barley, the youngest fully expanded leaf was excised at its base.
211 The leaf was then recut just above the initial excision under water and transferred under
212 water to a 15ml falcon tube. For maize, the youngest fully expanded leaf was excised at its
213 base, recut just above the initial excision under water and transferred under water to a 50ml
214 falcon tube. We ensured that all falcon tubes contained sufficient water so that the excision
215 point was consistently submerged. Excised leaves were left on the same lab bench as their
216 intact counterparts.

On the measurement day, excised and intact leaves were subject to a series of parallel measurements as highlighted in Supplemental Figure S1, with details provided below. Tomato plants were measured eight weeks post sowing across a two-day period. Barley plants were measured across two separate two-day periods one week apart, four and five weeks post sowing. Maize plants were measured across two separate two-day periods two weeks apart, six and eight weeks post sowing.

Leaf-level gas exchange

Leaf-level gas exchange measurements were performed using two LI-COR 6400XT infra-red gas analysers fitted with 6400-40 fluorometer LED light sources (LI-COR Biosciences, Lincoln, NE). To measure light-saturated gas exchange, conditions within the gas exchange chamber were set as follow: 25°C block temperature; 400 µmol s^{-1} air flow; 65-75% relative humidity (RH); 400 µmol s^{-1} reference CO_2 concentration; 1500 µmol m^{-2} s^{-1} PAR. Once A_N and g_s were stable, light saturated rates of gas exchange were logged before initiating a CO_2 response curve as described below.

For the tomato and barley CO_2 response curves, all conditions were kept as described above with gas exchange being measured at a series of reference CO_2 concentrations as follows: 400, 300, 200, 100, 50, 400, 400, 700, 1000, 1300, and 1800. Rates of gas exchange were logged at each point according to stability criteria waiting a minimum of 90 seconds and a maximum of 120 seconds at each point.

For the maize CO_2 response curves, all conditions were again kept as described for the light saturated gas exchange. Reference CO_2 was then increased in the following steps: 400, 600, 800, 1000, and 1250. Reference CO_2 was then returned to 400 and rates of A_N and g_s were allowed to re-stabilise before reducing reference CO_2 in the following sequence: 400, 300, 250, 200, 100, 75, and 25. Rates of gas exchange were logged at each point according to stability criteria waiting a minimum of 60 seconds and a maximum of 90 seconds at each point.

248 For tomato and barley, A_N-c_i data from the response curves were fit according to the FvCB
249 model (Farquhar *et al.*, 1980) using the fitacis() function from the R package plantecophys
250 (Duursma, 2015). This was achieved using the bilinear method to estimate the transition
251 point. From this, estimates of the maximum rate of Rubisco carboxylation (V_{cmax}) and the
252 maximum rate of electron transport for RuBP regeneration (J_{max}) on a C_i basis were obtained.
253 For maize, A_N-c_i data from the response curves were fit using a custom R function following
254 von Caemmerer, (2000). Here, the initial relationship between A_N and c_i was used to estimate
255 the maximum rate of carboxylation by PEPC (V_{pmax}). Additionally, the horizontal asymptote of
256 a four-parameter non-rectangular hyperbola was used as an estimate of CO_2- and light-
257 saturated photosynthesis (V_{max}).
258

259 **Hyperspectral reflectance**

260 Hyperspectral reflectance measurements were performed using an ASD FieldSpec 4 Standard-
261 Res Spectroradiometer equipped with a leaf-clip (Malvern Panalytical, Malvern, UK). The light
262 source of the FieldSpec was allowed to warm up for 45 minutes prior to measurements.
263 Hyperspectral reflectance was always measured on the same area of the leaf that gas
264 exchange was performed on and always with the light source pointing towards the adaxial
265 leaf surface. For each leaf, three technical replicates of hyperspectral reflectance were
266 performed within the spot used for gas exchange measurements. Reflectance at each
267 wavelength was then averaged across the three technical replicates for further data analyses.
268 These measurements were performed immediately following the CO_2-response gas exchange
269 measurements.
270

271 **Chlorophyll fluorescence**

272 Chlorophyll fluorescence measurements were performed using both the previously described
273 LICOR 6400XT leaf chamber fluorometer and using a closed chlorophyll fluorescence imaging
274 system (FluorCam FC 800-C, PSI, Czech Republic). For both, a similar program was designed
275 to measure the induction of non-photochemical quenching (NPQ) in response to actinic light
276 and the subsequent relaxation of NPQ following the actinic light being switched off.
277

278 Following the afternoon hyperspectral reflectance measurements, a portion of leaf was dark
279 adapted using aluminium foil for 45 minutes. After dark adaption, leaves were clamped within
280 the gas exchange chamber where conditions were as described previously except the light
281 source was switched off. Following estimation of dark-adapted maximum fluorescence (F_m),
282 the light source was switched on to 1500 µmol m^{-2} s^{-1} PAR for 10 minutes and a series of 12
283 saturating pulses were performed to estimate maximal fluorescence (F_m') at different time-
284 points. The light source was then subsequently switched off for 12 minutes and a further
285 series of eight saturating pulses were performed again to estimate F_m'. NPQ at each point of
286 measurement of chlorophyll fluorescence was then calculated as $(F_m-F_m')/F_m'$.
287
288 Samples for measurements of chlorophyll fluorescence in the closed system were first
289 analysed for leaf water potential using a Scholander pressure chamber (see below). For barley
290 and maize, leaf strips approximately 3cm x 5cm were taken from the middle portion of the
291 measured leaf and for tomato the same sized strip was from the measured terminal leaflet.
292 Leaf strips were arranged onto damp filter paper and encased between non-reflective glass
293 as per Ferguson *et al.*, (2020). These samples were then dark adapted overnight and
294 measured for NPQ induction and relaxation within the closed chlorophyll fluorescence system
295 following the same sequence of steps as described when using the LI-COR 6400 leaf chamber
296 fluorometer.
297
298 Using the NPQ data generated by both the leaf chamber fluorometer and the closed
299 fluorescence system, separate exponential models were fit to the light induction (Equation 1)
300 and dark relaxation (Equation 2) components.
301
302 Equation 1: $y = a * (1 - exp(-b * t)$
303 Equation 2: $y = a * \big(exp(-b * t)\big) + c$
304
305 For both equations a represents the amplitude of the induction or relaxation response (a_ind
306 and a_rel), b is the rate constant for the induction or relaxation of NPQ (b_ind and b_rel), c is
307 an offset to account for a non-zero intercept (relaxation only), t is the measurement time
308 point, and y is NPQ.
309

310 **Leaf water potential**

311 Measurements of leaf water potential were performed using a Scholander pressure chamber
312 (Model 600, PMS Instrument Company, OR, USA) following manufacturer instructions. For
313 intact leaves, a clean excision was made with a razor blade towards the base of the leaf for
314 maize and barley or the petiole for tomato before immediately sealing the leaf into the
315 chamber to measure the leaf water potential. For excised leaves, a new additional excision
316 was made 3cm above the cut from the previous day before immediately measuring leaf water
317 potential in the same manner.

318

319 **ABA analysis**

320 Separate plants were grown for analyses of leaf ABA concentration. Here, the plants were
321 grown, and leaves were excised in exactly the same manner as described in the "Plant
322 Material and Experimental Design" section. Barley and maize plants were measured five
323 weeks post sowing and tomato plants were measured eight weeks post sowing. Samples for
324 ABA concentration measurements were taken in the morning (10am). Each sample was taken
325 from the middle portion of the leaf or terminal leaflet taking care to avoid the midrib in barley
326 and maize. Samples were immediately flash frozen and subsequently analysed for ABA
327 concentration using a competitive ELISA kit (Phytodetek Immunoassay Kit for ABA, Agdia,
328 Elkhart, IN) following the manufacturer's instructions. The area of each sample was measured
329 before flash freezing, so that ABA concentration could be expressed on leaf area basis.

330

331 **Data processing and statistical analyses**

332 All statistical analyses were performed within the R environment (Reference). All figures were
333 generated using ggplot2 (Valero-Mora, 2010) and gridExtra with some pre-processing in
334 Affinity designer (Serif, Nottingham, UK).

335

336 We performed two-way repeated measures analysis of variance (ANOVA) comparison of
337 means tests to test for significance of the treatment (excised or intact), the time of
338 measurement (AM or PM), and their interaction (treatment by time) for all gas exchange-
339 associated traits. We performed one-sample t-tests to test for differences in leaf water
340 potential and the chlorophyll fluorescence associated traits between excised and intact leaves

for each species independently. The chlorophyll fluorescence traits measured using the gas exchange leaf chamber fluorometer and the closed chlorophyll fluorescence system were analysed independently as instrumental differences in sample conditioning, excitation wavelength as well as detection fore optics preclude direct comparisons.

The asdreader R package was used for managing the hyperspectral reflectance data following best practise outlined in Burnett *et al.*, (2021). Hyperspectral reflectance data were initially analysed through a spectra-wide approach where one-way ANOVA comparison of means tests were performed to test for differences in reflectance between excised and intact leaves at each wavelength from 250-3500nm. Separate tests were performed for each species and each time point, i.e., AM and PM. We calculated a Bonferroni significance threshold ($\alpha = 0.05$) to avoid identification of false positive results. It is worth noting that since there is covariation between wavelengths of a given spectra, this threshold is likely to be somewhat stringent. For visualisation purposes, we transformed the p-value associated with each wavelength by $-\log_{10}$.

We additionally used the same hyperspectral reflectance data to calculate multiple reflectance indices (Supplemental Table S1). We used these indices to perform repeated measures two-way ANOVA comparison of means tests separately for each species and as described previously to test for effects due to treatment, timepoint, and their interaction.

Results

Leaf water potential and ABA accumulation

At the end of the measurement day, we measured leaf water potential of all measured leaves (Figure 1, Supplemental Figure S1). For tomato and maize, we did not observe a significant effect of leaf excision on leaf water potential. However, for barley the leaf water potential of excised leaves showed a small but significant difference with that of the intact leaves (-0.193 and -0.237 MPa, respectively; Figure 1b).

370 Leaf ABA concentration in excised and intact leaves was measured in the morning after the
371 excision. For all three species, leaf excision did not result in a significant up- or down-
372 regulation in ABA accumulation relative to intact leaves at this timepoint (Figure 2).
373
374 ***Light saturated gas exchange***
375 Light-saturated gas exchange was logged prior to the initiation of the A_N-c_i response
376 measurements in the morning and the afternoon (Supplemental Figure S1, Figure 3). Across
377 all three species, leaf excision did not have a significant effect on A_N. The timing of the
378 measurement did have a significant effect on A_N for barley and maize, but not tomato. Here,
379 A_N reduced in the afternoon for barley and maize. This reduction in A_N was independent of
380 the treatment, where A_N declined in both intact and excised leaves (Figure 3e, i). Neither
381 treatment, time, nor their interaction had a significant effect on g_s for tomato (Figure 3b).
382 Time had a significant effect on g_s for barley, where it declined into the afternoon as per A_N
383 (Figure 3f). The excision treatment did have a significant effect on *gs* for maize, where it was
384 reduced in excised leaves. Although the treatment by time interactive effect for g_s was not
385 significant, the difference between excised and intact leaves did appear to increase into the
386 afternoon (Figure 3j). We did not detect a significant effect of treatment, time, or their
387 interaction on c_i for barley (Figure 3g). However, for tomato, c_i increased significantly in the
388 afternoon for excised and intact leaves (Figure 3c). For maize, all tested independent variables
389 had a significant effect on c_i. Intact leaves demonstrated higher c_i than excised leaves in the
390 morning and the afternoon, but the difference increased in the afternoon (Figure 3k).
391 Significant effects on *iWUE* mirrored those observed for c_i, such that it significantly declined
392 in the afternoon for both tomato and maize, and it was significantly increased in excised
393 leaves of maize (Figure 5d, l). With respect to the diurnal effect on *iWUE* and c_i for maize, it is
394 worth noting that the changes into the afternoon are much stronger in intact leaves, i.e.,
395 *iWUE* and c_i are more stable across the day in excised leaves.
396
397 ***Photosynthetic capacity***
398 We modelled A_N-c_i response measurements to estimate photosynthetic capacity in the
399 morning and the afternoon of the three species (Supplemental Figure S1, Figure 4). Across
400 the three species, time had a significant effect on all modelled parameters except V_{pmax} in
401 maize (Figure 4k). In all other cases, the photosynthetic capacity parameters declined into the

402 afternoon regardless of whether the leaf being measured was excised or intact (Figure 4c, d,
403 g, h, l). We only detected one significant treatment effect, where V_{cmax} was significantly
404 reduced in excised barley leaves, however the reduction appeared relatively minor (Figure
405 4g). In addition, the p-value associated with the treatment effect for V_{pmax} in maize was close
406 to the traditional 5% significance threshold (Figure 4k). For all traits and species, we did not
407 observe a significant interaction effect of treatment and time, suggesting that any observed
408 effects were temporally consistent (Figure 4).
409
410 ***Leaf reflectance***
411 Hyperspectral reflectance was measured following the A_N-c_i response measurements in the
412 morning and the afternoon (Supplemental Figures S1, S2). None of the specific wavelengths
413 showed any difference in reflectance between excised and intact leaves in the morning or the
414 afternoon for any species according to the Bonferroni significance threshold (Figure 5).
415 Despite the lack of significant wavelength-treatment associations, it is still interesting to
416 observe the distinct species-specific patterns in spectra-wide reflectance differences between
417 the treatments which can be interpreted based on the dominant factors that are known to
418 control leaf reflectance across the hyperspectral range. The pattern of p-values across the
419 spectral range were similar in the morning and the afternoon for tomato (Figure 5a-b) and
420 maize (Figure 5e-f), however the pattern was distinctly different across these time points for
421 barley (Figure 5c-d). For tomato, p-values showed a general trend of decreasing (inverse for -
422 $\log_{10}$(p-values)) from 300 to 1800nm before increasing between 1800 and 1900nm. After this,
423 they decreased to roughly what they were before the increase before increasing again toward
424 the end of the spectral range (Figure 5a-b). This pattern suggests potential differences in leaf
425 water status between the excised and intact tomato leaves. For maize, the pattern of p-values
426 across the spectral range partially-resembled the pattern of reflectance (Figure 5e-f;
427 Supplemental Figure S2). Here, there was a broad peak of low p-values between 600 and
428 1400nm and a narrower peak between 1500 and 1800nm. Here, the initial peak may reflect
429 differences in leaf structure and the secondary peak is often associated with differences in
430 leaf water status. For barley in the morning, the pattern of p-values across the spectral range
431 was similar to that of maize reflecting potential effects of excision on leaf structure and water
432 absorption (Figure 5c, e, f). However, the initial portion of the range was also characterised
433 by comparatively reduced p-values, especially around 400nm (Figure 5c), which may suggest

434 an effect on the absorption of light by chlorophyll b. In the afternoon, the broad peak of low
435 p-values between 600 and 1400nm disappeared, but there were still minor peaks between
436 600 and 700nm and between 1800 and 2000nm (Figure 5d), suggesting potential minor
437 effects on chlorophyll absorption and water status respectively.
438
439 Using the hyperspectral reflectance data (Supplemental Figure S2), we additionally calculated
440 reflectance indices related to nitrogen status, chlorophyll content and leaf water status
441 (Supplemental Table S1). We examined how these were affected by leaf excision and time of
442 measurement, i.e., AM and PM (Supplemental Figure S1), via two-way repeated measures
443 ANOVA tests as per the previously described photosynthesis traits (Supplemental Figures S4-
444 6). Although this approach did find some significant differences, the observed effects were
445 minor in all cases.
446
447 For tomato, we did not observe any significant treatment, time, or treatment by time
448 interactions for any of the reflection indices. (Supplemental Figures S3). For barley, we
449 observed a significant time effect for the Datt Index, which is a proxy of total chlorophyll
450 content, where it was higher in the afternoon (Supplemental Figure S4b). For barley, we also
451 observed a significant interactive effect for the moisture stress index (MSI), which is an
452 inverted proxy for water content, where excised leaves had a higher MSI in the morning only,
453 which suggest their water content was reduced compared to intact leaves at this point but
454 not again in the afternoon (Supplemental Figure S4d). For maize, the only significant effect
455 observed was a treatment effect for the Datt Index, which was marginally higher in intact
456 leaves compared to excised leaves suggesting chlorophyll content was reduced following leaf
457 excision (Figure S5b) .
458
459 ***Chlorophyll fluorescence***
460 Chlorophyll fluorescence was measured using the leaf chamber fluorometer that was paired
461 to the gas exchange platform and on the subsequent day using the closed chlorophyll
462 fluorescence system (Supplemental Figure S1). We tested for significant differences between
463 samples taken from excised and intact leaves for F_v/F_m, the rates of induction and relaxation
464 of NPQ (b_ind and b_rel), and maximum NPQ. For the samples measured using the closed
465 chlorophyl fluorescence system, we did not observe a significant difference for any of these

466 four parameters (Figure 6). This was true for all of these same parameters as measured in the
467 leaf chamber fluorometer, expect for tomato b_ind, which was observed to be significantly
468 faster in intact versus excised leaves (Supplemental Figure S6b). It is worth noting that the p-
469 values associated with the one-sample t-tests comparing excised and intact tomato leaves for
470 F_v/F_m and maximum NPQ were close to the traditional 0.05 significance threshold (0.07 and
471 0.09 respectively), where intact leaves appeared to have higher photosystem II maximum
472 efficiency and light adapted NPQ (Supplemental Figure S5b).
473

474 # Discussion

475 Screening variation in photosynthetic traits across large numbers of genotypes is a key
476 requirement for targeting photosynthesis for crop improvement. Large-scale screening to this
477 end is fraught with logistical challenges that are commonly circumvented via phenotyping
478 excised leaf material (See: Introduction). A common limitation of these studies is the lack of
479 evidence highlighting the representative nature of such phenotyping, which accordingly
480 represents a key knowledge gap for this field. To this end, the principal aim of this study was
481 to ascertain if photosynthetic parameters measured on excised leaves were representative of
482 the same parameters measured on intact leaves in tomato, barley, and maize. There are at
483 least three studies that have attempted to quantify potential differences in non-crop species.
484 Using the Japanese stone oak (*Lithocarpus edulis*) evergreen tree species, Miyazawa *et al.*,
485 (2011) showed that multiple photosynthetic parameters demonstrated no significant
486 differences when measured on excised leaves relative to intact leaves. Here, the only trait
487 that did demonstrate a significant difference was stomatal conductance, which was
488 significantly higher in excised leaves. Despite this difference, the authors showed that it was
489 possible to use data from excised leaves to parametrise an ecophysiological model to
490 reproduce diurnal patterns of *in situ* gas exchange. In a similar study, Akalusi *et al.*, (2021)
491 showed there to be negligible differences in light saturated rates of gas exchange and
492 modelled estimates of photosynthetic capacity between excised and intact leaves of balsam
493 fir (*Abies balsamea*). Moreover, the authors also demonstrated that the non-significant
494 differences between these measurement types carried through across the growing season. In
495 contrast to these two studies, Richardson and Berlyn (2002) focused on how spectral
496 reflectance and chlorophyll fluorescence parameters were impacted by leaf excision in four

497 temperate tree species. They observed that spectral and chlorophyll fluorescence changes
498 were only minor at 12-hours post excision. Furthermore, they demonstrated that with
499 appropriate handling to maintain leaf water status, representative data could be obtained
500 from excised leaves as late as three days-post excision depending on the species. These
501 studies have demonstrated the effectiveness of phenotyping traits related to photosynthesis
502 on detached leaves of perennial woody species. As we highlight in the introduction, a similar
503 approach is now commonly employed for many crop studies. The numerous differences that
504 distinguish herbaceous annuals from trees suggest that the success of this approach may not
505 carry over to crop species, thereby highlighting the timeliness of this present study. Our
506 findings here largely provide long overdue experimental justification for applying this
507 approach on three major crop species, representing the major monocots and dicot groups as
508 well as C4 and C3 photosynthesis. The lack of large effects due to excision, as well as the
509 occurrence of some small but significant effects will be discussed in more detail in the next
510 sections.
511
512 ***Stabilised leaf water potential and ABA accumulation underlie the utility of phenotyping***
513 ***photosynthesis in excised leaves***
514 The most important crop species for staple foods are herbaceous annuals. A key anatomical
515 difference between woody and herbaceous species is the composition of xylem tissue.
516 Primary xylem is the only form of xylem for most herbaceous plants, including cereals (Růžička
517 *et al.*, 2015), although tomato can demonstrate a small amount of secondary xylem (Qi *et al.*,
518 2020). While primary xylem comprises a relatively thin central zone within stems and leaves,
519 secondary xylem grows out and differentiates from the vascular cambium (Kirst *et al.*, 2004).
520 Secondary xylem serves multiple purposes beyond facilitating water transport, including
521 biomechanical support and protection against physical damage (Sperry, 2003; Morris *et al.*,
522 2016; Miodek *et al.*, 2021). Avoiding xylem damage is critical for maintaining hydraulic
523 conductivity and protecting photosynthesis. Breakage of the water column through xylem
524 cavitation can disrupt this. Our results are supportive of the notion that the transpiration
525 stream of excised tomato, barley, and maize leaves is maintained following recutting them
526 underwater as we did not observe negative effects on leaf water status measured as leaf
527 water potential (Figure 1). The utility of performing photosynthesis on excised leaves from
528 woody species may be supported by the presence of secondary xylem tissue, since these

529 measurements are typically performed by excising woody branches attached to leaves of
530 interest. Furthermore, vulnerability segmentation work has shown that branches are more
531 resistant to xylem cavitation than terminal leaves (Zhu *et al.*, 2016). Stem and leaf hydraulic
532 conductance are coordinated (Pivovaroff *et al.*, 2014), therefore excising leaves may remove
533 the association of leaf and stem hydraulic conductance. It is plausible that the reduction in
534 leaf water potential of intact barley leaves (Figure 1b) is a function of this and that by
535 detaching the leaf from the stem and immersing it in water, this process increases water
536 availability by removing the hydraulic resistance imposed by the stem. Alternatively, this
537 difference may suggest that the plants attached to the measured leaves were marginally
538 water stressed, however this is unlikely given the absolute water potential values were
539 greater than -0.25MPa since we ensured that all plants were well-watered throughout
540 growing and on the day before measurements. Moreover, the barley light-saturated gas
541 exchange data did not demonstrate a signal of water stress in the intact leaves relative to the
542 excised leaves (as discussed below). In general, the values for water potential obtained here
543 and the minor difference between excised and intact leaves suggests a lack of water stress.
544
545 It has been suggested that roots are essential for stimulating ABA biosynthesis in leaves
546 (Takahashi *et al.*, 2018), however many studies that involve work with excised leaves have
547 demonstrated that ABA levels can increase independently of roots (Bauer *et al.*, 2013;
548 Sussmilch *et al.*, 2017; McAdam and Brodribb, 2018). It is therefore plausible that any
549 treatment effects observed as a result of leaf excision could be imparted due to foliar ABA
550 accumulation. Depending on the site and method of excision, the act of cutting a leaf or a
551 tiller from a plant may elicit a wounding-type response. ABA can accumulate in response to
552 wounding as a regulator of downstream defense mechanisms (Cui *et al.*, 2013; Savatin *et al.*,
553 2014). Additionally, the process of excision is likely to impair xylem tension influencing the
554 flow rate of water to the leaf. This may also result in ABA accumulation in the leaf to stabilise
555 leaf water status by reducing transpiration, however there no evidence presently exists to
556 support this notion. Moreover, it is likely that the subsequent recutting of leaves underwater
557 as per this study and other studies will quickly re-establish xylem tension by mitigating against
558 cavitation. The role of ABA in regulating ion transport into guard cells to induce stomatal
559 closure is well characterised (Schroeder *et al.*, 2001), consequently if leaf excision were to
560 induce leaf ABA accumulation through any basis, we could expect to see associated

561 reductions in gas exchange as result of stomatal closure. To this end, our results
562 demonstrated that in the morning following leaf excision there was no significant difference
563 in the leaf ABA concentration between intact and excised leaves in either of three species
564 (Figure 2). Performing leaf excision on the day prior to phenotyping was premeditated as we
565 hypothesised that this would allow sufficient time for degradation of any additionally
566 accumulated ABA. So, while our results do not allow us to determine whether excision
567 stimulates an immediate ABA response, they are supportive of a lack of differential
568 accumulation of ABA in leaves that are excised on the day prior to measurements.
569 Consequently, we recommend adopting this approach when phenotyping excised leaves to
570 avoid any confounding effects that may potentially arise due to ABA accumulation.
571
572 ***Differences between excised and intact leaves for gas exchange traits are limited, but***
573 ***important and species-specific***
574 Our methodology of leaf excision mirrors a widespread approach utilised by many research
575 groups for performing photosynthesis-related phenotyping of material that is difficult to
576 measure *in-situ* for a multitude of reasons. This approach is ultimately necessary and defines
577 the ability to perform large scale screening of diversity that is important to characterise.
578 Despite this, leaf excision may represent a significant shock to the leaf and plausibly elicit
579 substantial wounding responses. Prior to this study, little data existed to support the
580 efficiency of this approach for generating data matching that obtained from intact leaves. To
581 this end, perhaps the most critical finding of our study is that we did not observe a significant
582 effect of leaf excision on A_N. This was true for all three species tested and across the morning
583 and afternoon measurements (Figure 3a, e, i). This is an important finding and goes a long
584 way to highlight the utility of this approach for assessing light-saturated photosynthesis at
585 ambient CO_2. While we did not observe significant treatment effects on A_N, we did observe
586 significant time of measurement effects for barley and maize, where A_N declined into the
587 afternoon (Figure 1e, i). This is indicative of the diurnal pattern of photosynthesis where, in
588 many species, there is a decline in A_N into the afternoon (Singsaas *et al.*, 2000; Mohotti and
589 Lawlor, 2002; Ainsworth *et al.*, 2007; Koester *et al.*, 2016; Vialet-Chabrand *et al.*, 2017). This
590 can be attributed to multiple factors including declining electron transport and changes to
591 the apparent sink strength due to increasing leaf carbohydrate content (Singsaas *et al.*, 2000;
592 Koester *et al.*, 2016). So, while this excision approach is supportive of phenotyping A_N, our

593 findings suggest that interpreting and comparing data obtained across an extended diurnal
594 period necessitates caution regardless of whether it was collected from intact or excised
595 leaves.
596
597 A further, and curious, significant time of day effect was detected for c_i in tomato (Figure 3c).
598 Here, c_i increased into the afternoon for both treatments despite no significant changes in A_N
599 or g_s that could be presupposed to lead to increases in c_i. This result may be a function of
600 lower Rubisco activity, which is suggested by declining V_{cmax} in tomato for both treatments
601 into the afternoon (Figure 4c). Here, lower carboxylation by Rubisco may lead to an increase
602 in CO_2 in the intracellular air space of the leaf in the afternoon compared to the morning,
603 especially since g_s was not observed to change across these time periods. This result highlights
604 the importance of quantifying photosynthetic capacity to generate a broader picture of the
605 photo-physiological state of the leaf, as opposed to relying on light-saturated measurements
606 made under ambient CO_2. Declining V_{cmax} in the afternoon for tomato here may be a function
607 of the diurnal expression patterns of Rubisco activase (Rca). Rca is the molecular chaperone
608 that defines Rubisco activity, and its expression has been demonstrated to decline
609 significantly into the afternoon (Perdomo *et al.*, 2021). The afternoon decline in tomato *iWUE*
610 (Figure 3d) mirrors the increase in c_i (Leakey *et al.*, 2019) and is a function of the combination
611 of the decline in A_N (Figure 3b) and increase in g_s (Figure 3c), despite those changes being
612 non-significant in isolation.
613
614 One of the more surprising results from our study was that maize was the only one of the
615 three species where we detected a treatment effect on g_s (Figure 3j). Here, the excision
616 process resulted in a significant decline in g_s compared to intact leaves. This result is
617 somewhat surprising since maize leaves are larger and appear more physically robust than
618 barley leaves and the petiole of tomato leaves. Nevertheless, we ascribe confidence to this
619 result since it was consistent across the two time points, therein highlighting the impairing
620 influence of leaf excision on stomatal opening in maize. The C_4 carbon concentrating
621 mechanism that defines the relative de-coupling of g_s and A_N in C_4 species relative to C_3
622 species (Leakey *et al.*, 2019) may underly why we do not observe a concurrent treatment
623 effect on A_N in maize. Namely, the decrease in g_s observed in the excised leaves was not
624 sufficient to decrease c_i enough to lose CO_2 saturation of A_N (Figure k) as evident from the

625 A_N/c_i responses (Figure 3j). The treatment effect of leaf excision on g_s in maize but not on A_N,
626 led to expected results for c_i, where it decreased significantly at both time points due to
627 decreased capacity for CO_2 uptake (Figure 3k). Concurrently, the stomatal resistance to water
628 loss was greater, such that *iWUE* was higher at both time points and more so again in the
629 afternoon (Figure 3l). Taken together, these results show that the time-of-day effects on light-
630 saturated rate of gas exchange are stronger in intact maize leaves, thereby highlighting the
631 potential for longer measurement days when working with excised leaves.
632
633 Despite the above-described differences observed in maize, we did not observe any
634 significant effects in terms of treatment or time on the photosynthetic capacity traits, namely
635 V_{pmax} and V_{max} (Figure 2k, l). This suggests that reduced g_s at the starting point of the A_N-c_i
636 response measurements, i.e., ambient CO_2, in excised leaves did not compromise the ability
637 to assess the rate of photosynthetic induction from low-to-ambient CO_2 concentrations or the
638 rates of photosynthesis when g_s is minimal at high CO_2 concentrations. Our results are
639 therefore supportive of performing A_N-c_i response curves in excised maize leaves to model
640 photosynthetic capacity. In general, our results are also supportive of performing A_N-c_i
641 response curves on excised leaves of the C_3 species. We did detect significant reductions in
642 V_{cmax} (barley; Figure 4g) but the difference was minor and not exaggerated by the interaction
643 with time.
644
645 ***Reflectance and chlorophyll fluorescence appear relatively unchanged between intact and***
646 ***excised leaves***
647 There were no statistically significant differences detected for leaf reflectance between the
648 treatments for any of the species on a wavelength-by-wavelength basis (Figure 5). Despite
649 this, the pattern of p-values across the spectrum were surprisingly unique between the
650 species and different between the time points for barley. In general, if we consider the
651 dominant factors that influence leaf reflectance (Kokaly *et al.*, 2003), the p-value patterns
652 suggest the most excision-sensitive aspects of reflectance were due to leaf water content in
653 tomato and light scattering in the mesophyll in barley and maize (Figure 5). The results from
654 barley and maize here are similar to those observed across certain tree species by Richardson
655 and Berlyn, (2002), where the authors and others suggest reductions in near-infra red spectra
656 reflectance in excised leaves are related to leaf structural changes at the cellular level. Here,

657 declining leaf water status results in cytoplasmic shrinkage, such that light scattering alters at
658 the interface between cell walls and water (Carter, 1991; Aldakheel and Danson, 1997;
659 Richardson and Berlyn, 2002). However, we do not observe perturbed leaf water status in
660 excised leaves (Figure 1), consequently this may reflect why the patterns we highlight in terms
661 of differences in reflectance between the treatments do not pass significance thresholds
662 (Figure 5). The study of Richardson and Berlyn, (2002) tested differences between excised and
663 intact leaves over several days post-excision and did not begin to detect significant differences
664 in reflectance indices and chlorophyll fluorescence until 48 hours after excision.
665 Consequently, it is possible that we may have observed differences in reflectance and other
666 traits had we measured for a further day, however this is not common practice with crop
667 species, and we would advise against this.
668
669 To resolve any potential reflectance differences between intact and excised leaves, we
670 calculated five commonly employed reflectance indices (Supplemental Table S1,
671 Supplemental Figures S3-5). In doing so, we were only able to detect two statistically
672 significant differences between intact and excised leaves. For barley, the MSI was significantly
673 higher in the morning in excised leaves suggesting a reduction in leaf water content, however
674 this effect was not apparent in the afternoon (Supplemental Figure S4d). In maize, a
675 significant treatment effect on the Datt index, which is positively correlated to chlorophyll
676 content (Lu *et al.*, 2015), suggested that chlorophyll content was reduced in excised leaves
677 (Supplemental Figure S5b). Here, it could be hypothesised that ABA accumulation would be
678 an the underlying mechanism resulting in this difference, since there is also some evidence
679 linking leaf yellowing and reductions in leaf chlorophyll to ABA, however that is evidently not
680 the situation in our study (Figure 2) and this is typically a longer-term effect (Wang *et al.*,
681 2018). In general, our results here suggest that reflectance changes between excised and
682 intact leaves are slight, which is similar to what has previously been shown in woody species
683 (Richardson and Berlyn, 2002).
684
685 Our results also mirror those of Richardson and Berlyn, (2002) in that we saw no differences
686 in F_v/F_m in either of methods through which it was assessed in this study (Figure 6 and
687 Supplemental Figure S6). This highlights how electron flow in PSII is not significantly impacted
688 by this approach, so there is no impairment on the photosynthetic apparatus. In our study we

also demonstrated no significant differences in the dynamics of NPQ, expect for a minor reduction in the rate of induction in excised tomato leaves when measured using the gas exchange leaf chamber fluorometer (Supplemental Figure S6a). The fact that this was not detected the following day using the closed chlorophyll fluorescence system suggests that this is more likely to result from insufficient time allowed for dark adaption, especially since F_v/F_m was also bordering on being significantly reduced in excised leaves when measured in the leaf chamber fluorometer also ($p = 0.07$; Supplemental Figure S6a).

Conclusion

Screening large amounts of diversity for photosynthesis-related traits is only realistically possible with excised leaves. Therefore, the evidence presented in this study that validates this approach, in terms of its affiliation to intact-leaf measurements, is welcomed. Despite this, our study does highlight the existence of specifies-specific treatment effects, e.g., g_s reduction in maize, that the community should be aware of. Moreover, this should encourage those who are planning on adopting this approach to validate if it is suitable for their species of interest. One salient point that our study does not address is the potential for differential responses to excision on an intra-specific basis. An obvious further extension to this study would be to test how genetically distinct genotypes within a species perform following leaf excision as this has the potential to have large consequences for studies of this nature.

Supplemental Material

Supplemental Figure S1. Overview of experimental workflow.

Supplemental Figure S2. Mean hyperspectral reflectance data. The solid line represents the mean reflectance, and the shaded area represents the standard error of the mean. (a) Tomato AM (b) Tomato PM (c) Barley AM (d) Barley PM (e) Maize AM (f) Maize PM

Supplemental Figure S3. Hyperspectral reflectance derived indices for tomato. (a) Red Edge-Normalised Difference Vegetation Index (RE-NDVI), (b) Datt Index (c) Normalised Difference Nitrogen Index (NDNI), (d) Moisture Stress Index (MSI), and (e) Leaf Water Index (LWI)

720 Supplemental Figure S4. Hyperspectral reflectance derived indices for barley. (a) Red Edge-
721 Normalised Difference Vegetation Index (RE-NDVI), (b) DATT Index (c) Normalised Difference
722 Nitrogen Index (NDNI), (d) Moisture Stress Index (MSI), and (e) Leaf Water Index (LWI)
723
724 Supplemental Figure S5. Hyperspectral reflectance derived indices for maize. (a) Red Edge-
725 Normalised Difference Vegetation Index (RE-NDVI), (b) DATT Index (c) Normalised Difference
726 Nitrogen Index (NDNI), (d) Moisture Stress Index (MSI), and (e) Leaf Water Index (LWI)
727
728 Supplemental Figure S6. Boxplots showing variation in chlorophyll fluorescence associated
729 traits between excised and intact leaves measured using the leaf chamber fluorometer.
730
731 Supplemental Table S1. Reflectance indices used in this study.
732

733 Acknowledgments

734 This work was supported by the European Union's Horizon2020 research and innovation
735 programme (No.862201) project CAPITALISE. We thank Dr Cristina Sales and Dr Angie Burnett
736 for assistance in generating the ABA data. We thank Dr Sara Lopez-Gomollon for providing
737 the tomato seed. We thank Katie Shaw for assistance in performing the modelling of the
738 chlorophyll fluorescence data and Prof Howard Griffiths and Dr Jessica Royles for assistance
739 with the leaf water potential measurements. For the purpose of open access, the authors
740 have applied a Creative Commons Attribution (CC BY) licence to any Author Accepted
741 Manuscript version arising from this submission.
742

743 Author contributions

744 JNF, TL and JK designed the study. JNF and TJ carried out the experiments. JNF and TJ
745 performed the data analyses. All authors helped to interpret the results. JNF and JK wrote the
746 paper with input from all the authors.
747

748 Conflict of interest

749 The authors have no conflicts of interest to declare.

References

Ainsworth EA, Long SP. 2021. 30 years of free-air carbon dioxide enrichment (FACE): What have we learned about future crop productivity and its potential for adaptation? Global Change Biology **27**, 27–49.

Ainsworth EA, Rogers A, Leakey ADB, Heady LE, Gibon Y, Stitt M, Schurr U. 2007. Does elevated atmospheric [CO2] alter diurnal C uptake and the balance of C and N metabolites in growing and fully expanded soybean leaves? Journal of Experimental Botany **58**, 579–591.

Akalusi ME, Meng F, P.-A. Bourque C. 2021. Photosynthetic parameters and stomatal conductance in attached and detached balsam fir foliage. Plant-Environment Interactions **2**, 206–215.

Aldakheel YY, Danson FM. 1997. Spectral reflectance of dehydrating leaves: Measurements and modelling. International Journal of Remote Sensing **18**, 3683–3690.

Bauer H, Ache P, Lautner S, *et al.* 2013. The stomatal response to reduced relative humidity requires guard cell-autonomous ABA synthesis. Current biology: CB **23**, 53–57.

Beardsell MF, Cohen D. 1975. Relationships between Leaf Water Status, Abscisic Acid Levels, and Stomatal Resistance in Maize and Sorghum. Plant Physiology **56**, 207–212.

Blatt MR. 2000. Cellular signaling and volume control in stomatal movements in plants. Annual Review of Cell and Developmental Biology **16**, 221–241.

Burnett AC, Anderson J, Davidson KJ, Ely KS, Lamour J, Li Q, Morrison BD, Yang D, Rogers A, Serbin SP. 2021. A best-practice guide to predicting plant traits from leaf-level hyperspectral data using partial least squares regression (T Lawson, Ed.). Journal of Experimental Botany **72**, 6175–6189.

von Caemmerer S. 2000. *Biochemical Models of Leaf Photosynthesis*. CSIRO Publishing.

Canny M. 1997. Vessel contents of leaves after excision - a test of Scholander's assumption. American Journal of Botany **84**, 1217.

Carmo-Silva E, Andralojc PJ, Scales JC, Driever SM, Mead A, Lawson T, Raines CA, Parry MAJ. 2017. Phenotyping of field-grown wheat in the UK highlights contribution of light response of photosynthesis and flag leaf longevity to grain yield. Journal of Experimental Botany **68**, 3473–3486.

Carter GA. 1991. Primary and Secondary Effects of Water Content on the Spectral Reflectance of Leaves. American Journal of Botany **78**, 916–924.

Chen D, Wang S, Xiong B, Cao B, Deng X. 2015. Carbon/Nitrogen Imbalance Associated with Drought-Induced Leaf Senescence in Sorghum bicolor. PLOS ONE **10**, e0137026.

Choquette NE, Ogut F, Wertin TM, Montes CM, Sorgini CA, Morse AM, Brown PJ, Leakey ADB, McIntyre LM, Ainsworth EA. 2019. Uncovering hidden genetic variation in

787 photosynthesis of field-grown maize under ozone pollution. Global Change Biology **25**,
788 4327–4338.

789 **Collison RF, Raven EC, Pignon CP, Long SP**. 2020. Light, Not Age, Underlies the
790 Maladaptation of Maize and Miscanthus Photosynthesis to Self-Shading. Frontiers in Plant
791 Science **11**, 783.

792 **Cui F, Brosché M, Sipari N, Tang S, Overmyer K**. 2013. Regulation of ABA dependent
793 wound induced spreading cell death by MYB 108. New Phytologist **200**, 634–640.

794 **De Souza AP, Burgess SJ, Doran L, Hansen J, Manukyan L, Maryn N, Gotarkar D,**
795 **Leonelli L, Niyogi KK, Long SP**. 2022. Soybean photosynthesis and crop yield are
796 improved by accelerating recovery from photoprotection. Science **377**, 851–854.

797 **Driever SM, Lawson T, Andralojc PJ, Raines CA, Parry MAJ**. 2014. Natural variation in
798 photosynthetic capacity, growth, and yield in 64 field-grown wheat genotypes. Journal of
799 Experimental Botany **65**, 4959–4973.

800 **Driever SM, Simkin AJ, Alotaibi S, Fisk SJ, Madgwick PJ, Sparks CA, Jones HD,**
801 **Lawson T, Parry MAJ, Raines CA**. 2017. Increased SBPase activity improves
802 photosynthesis and grain yield in wheat grown in greenhouse conditions. Philosophical
803 Transactions of the Royal Society B: Biological Sciences **372**, 20160384.

804 **Duursma RA**. 2015. Plantecophys - An R Package for Analysing and Modelling Leaf Gas
805 Exchange Data. PLOS ONE **10**, e0143346.

806 **Farquhar GD, von Caemmerer S, Berry JA**. 1980. A biochemical model of photosynthetic
807 CO2 assimilation in leaves of C 3 species. Planta **149**, 78–90.

808 **Ferguson JN, Fernandes SB, Monier B, *et al.*** 2021. Machine learning-enabled phenotyping
809 for GWAS and TWAS of WUE traits in 869 field-grown sorghum accessions. Plant
810 Physiology **187**, 1481–1500.

811 **Ferguson JN, McAusland L, Smith KE, Price AH, Wilson ZA, Murchie EH**. 2020. Rapid
812 temperature responses of photosystem II efficiency forecast genotypic variation in rice
813 vegetative heat tolerance. The Plant Journal: For Cell and Molecular Biology **104**, 839–855.

814 **Gojon A, Nussaume L, Luu DT, *et al.*** 2023. Approaches and determinants to sustainably
815 improve crop production. Food and Energy Security **12**.

816 **Govindjee, Downton WJS, Fork DC, Armond PA**. 1981. Chlorophyll A fluorescence
817 transient as an indicator of water potential of leaves. Plant Science Letters **20**, 191–194.

818 **Kirst M, Myburg AA, De León JPG, Kirst ME, Scott J, Sederoff R**. 2004. Coordinated
819 Genetic Regulation of Growth and Lignin Revealed by Quantitative Trait Locus Analysis of
820 cDNA Microarray Data in an Interspecific Backcross of Eucalyptus. Plant Physiology **135**,
821 2368–2378.

822 **Koester RP, Nohl BM, Diers BW, Ainsworth EA**. 2016. Has photosynthetic capacity
823 increased with 80 years of soybean breeding? An examination of historical soybean cultivars.
824 Plant, Cell & Environment **39**, 1058–1067.

825 **Kokaly RF, Despain DG, Clark RN, Livo KE**. 2003. Mapping vegetation in Yellowstone
826 National Park using spectral feature analysis of AVIRIS data. Remote Sensing of
827 Environment **84**, 437–456.

828 **Kromdijk J, Long SP**. 2016. One crop breeding cycle from starvation? How engineering
829 crop photosynthesis for rising CO_2 and temperature could be one important route to
830 alleviation. Proceedings of the Royal Society B: Biological Sciences **283**, 20152578.

831 **Leakey ADB, Ferguson JN, Pignon CP, Wu A, Jin Z, Hammer GL, Lobell DB**. 2019.
832 Water Use Efficiency as a Constraint and Target for Improving the Resilience and
833 Productivity of C3 and C4 Crops. Annual Review of Plant Biology **70**, 781–808.

834 **Leakey ADB, Uribelarrea M, Ainsworth EA, Naidu SL, Rogers A, Ort DR, Long SP**.
835 2006. Photosynthesis, Productivity, and Yield of Maize Are Not Affected by Open-Air
836 Elevation of CO2 Concentration in the Absence of Drought. Plant Physiology **140**, 779–790.

837 **Lenaerts B, Collard BCY, Demont M**. 2019. Review: Improving global food security
838 through accelerated plant breeding. Plant Science **287**, 110207.

839 **Liao Q, Gu S, Kang S, Du T, Tong L, Wood JD, Ding R**. 2022. Mild water and salt stress
840 improve water use efficiency by decreasing stomatal conductance via osmotic adjustment in
841 field maize. Science of The Total Environment **805**, 150364.

842 **Long SP**. 2003. Gas exchange measurements, what can they tell us about the underlying
843 limitations to photosynthesis? Procedures and sources of error. Journal of Experimental
844 Botany **54**, 2393–2401.

845 **Lu S, Lu X, Zhao W, Liu Y, Wang Z, Omasa K**. 2015. Comparing vegetation indices for
846 remote chlorophyll measurement of white poplar and Chinese elm leaves with different
847 adaxial and abaxial surfaces. Journal of Experimental Botany **66**, 5625–5637.

848 **Makino A, Shimada T, Takumi S, Kaneko K, Matsuoka M, Shimamoto K, Nakano H,**
849 **Miyao-Tokutomi M, Mae T, Yamamoto N**. 1997. Does Decrease in Ribulose-1,5-
850 Bisphosphate Carboxylase by Antisense RbcS Lead to a Higher N-Use Efficiency of
851 Photosynthesis under Conditions of Saturating CO2 and Light in Rice Plants? Plant
852 Physiology **114**, 483–491.

853 **Markelz RJC, Strellner RS, Leakey ADB**. 2011. Impairment of C4 photosynthesis by
854 drought is exacerbated by limiting nitrogen and ameliorated by elevated [CO2] in maize.
855 Journal of Experimental Botany **62**, 3235–3246.

856 **McAdam SAM, Brodribb TJ**. 2018. Mesophyll Cells Are the Main Site of Abscisic Acid
857 Biosynthesis in Water-Stressed Leaves. Plant Physiology **177**, 911–917.

858 **McAusland L, Atkinson JA, Lawson T, Murchie EH**. 2019. High throughput procedure
859 utilising chlorophyll fluorescence imaging to phenotype dynamic photosynthesis and
860 photoprotection in leaves under controlled gaseous conditions. Plant Methods **15**, 109.

861 **McCormick AJ, Cramer MD, Watt DA**. 2008. Changes in Photosynthetic Rates and Gene
862 Expression of Leaves during a Source–Sink Perturbation in Sugarcane. Annals of Botany
863 **101**, 89–102.

Miodek A, Gizińska A, Włoch W, Kojs P. 2021. What do we know about growth of vessel elements of secondary xylem in woody plants? Biological Reviews **96**, 2911–2924.

Miyazawa Y, Tateishi M, Komatsu H, Kumagai T, Otsuki K. 2011. Are measurements from excised leaves suitable for modeling diurnal patterns of gas exchange of intact leaves? Hydrological Processes **25**, 2924–2930.

Mohotti AJ, Lawlor DW. 2002. Diurnal variation of photosynthesis and photoinhibition in tea: effects of irradiance and nitrogen supply during growth in the field. Journal of Experimental Botany **53**, 313–322.

Montes CM, Fox C, Sanz-Sáez Á, *et al.* 2022. High-throughput characterization, correlation, and mapping of leaf photosynthetic and functional traits in the soybean (*Glycine max*) nested association mapping population (T Juenger, Ed.). Genetics, iyac065.

Morcuende R, Kostadinova S, Pérez P, Martínez-Carrasco R. 2005. Fructan synthesis is inhibited by phosphate in warm-grown, but not in cold-treated, excised barley leaves. The New Phytologist **168**, 567–574.

Morgan PB, Bernacchi CJ, Ort DR, Long SP. 2004. An in vivo analysis of the effect of season-long open-air elevation of ozone to anticipated 2050 levels on photosynthesis in soybean. Plant Physiology **135**, 2348–2357.

Morris H, Plavcová L, Cvecko P, *et al.* 2016. A global analysis of parenchyma tissue fractions in secondary xylem of seed plants. New Phytologist **209**, 1553–1565.

Müllers Y, Postma JA, Poorter H, van Dusschoten D. 2022. Stomatal conductance tracks soil-to-leaf hydraulic conductance in faba bean and maize during soil drying. Plant Physiology **190**, 2279–2294.

Murchie EH, Chen Y, Hubbart S, Peng S, Horton P. 1999. Interactions between Senescence and Leaf Orientation Determine in Situ Patterns of Photosynthesis and Photoinhibition in Field-Grown Rice1. Plant Physiology **119**, 553–564.

Nguyen D, Rieu I, Mariani C, van Dam NM. 2016. How plants handle multiple stresses: hormonal interactions underlying responses to abiotic stress and insect herbivory. Plant Molecular Biology **91**, 727–740.

Perdomo JA, Buchner P, Carmo-Silva E. 2021. The relative abundance of wheat Rubisco activase isoforms is post-transcriptionally regulated. Photosynthesis Research **148**, 47–56.

Pivovaroff AL, Sack L, Santiago LS. 2014. Coordination of stem and leaf hydraulic conductance in southern C alifornia shrubs: a test of the hydraulic segmentation hypothesis. New Phytologist **203**, 842–850.

Qi X, Takahashi H, Kawasaki Y, *et al.* 2020. Differences in xylem development between Dutch and Japanese tomato (Solanum lycopersicum) correlate with cytokinin levels in hypocotyls. Annals of Botany **126**, 315–322.

Richardson AD, Berlyn GP. 2002. Changes in foliar spectral reflectance and chlorophyll fluorescence of four temperate species following branch cutting. Tree Physiology **22**, 499–506.

Růžička K, Ursache R, Hejátko J, Helariutta Y. 2015. Xylem development – from the cradle to the grave. New Phytologist **207**, 519–535.

Savatin DV, Gramegna G, Modesti V, Cervone F. 2014. Wounding in the plant tissue: the defense of a dangerous passage. Frontiers in Plant Science **5**.

Schroeder JI, Allen GJ, Hugouvieux V, Kwak JM, Waner D. 2001. GUARD CELL SIGNAL TRANSDUCTION. Annual Review of Plant Physiology and Plant Molecular Biology **52**, 627–658.

Singsaas EL, Ort DR, DeLUCIA EH. 2000. Diurnal regulation of photosynthesis in understory saplings: Diurnal regulation of photosynthesis. New Phytologist **145**, 39–49.

Sperry JS. 2003. Evolution of Water Transport and Xylem Structure. International Journal of Plant Sciences **164**, S115–S127.

Sussmilch FC, Brodribb TJ, McAdam SAM. 2017. Up-regulation of NCED3 and ABA biosynthesis occur within minutes of a decrease in leaf turgor but AHK1 is not required. Journal of Experimental Botany **68**, 2913–2918.

Takahashi F, Suzuki T, Osakabe Y, Betsuyaku S, Kondo Y, Dohmae N, Fukuda H, Yamaguchi-Shinozaki K, Shinozaki K. 2018. A small peptide modulates stomatal control via abscisic acid in long-distance signalling. Nature **556**, 235–238.

Tegeder M, Masclaux-Daubresse C. 2018. Source and sink mechanisms of nitrogen transport and use. The New Phytologist **217**, 35–53.

Tyree MT, Cochard H. 2003. Vessel contents of leaves after excision: a test of the Scholander assumption. Journal of Experimental Botany **54**, 2133–2139.

Valero-Mora PM. 2010. **ggplot2:** Elegant Graphics for Data Analysis. Journal of Statistical Software **35**.

Vialet-Chabrand SRM, Matthews JSA, McAusland L, Blatt MR, Griffiths H, Lawson T. 2017. Temporal Dynamics of Stomatal Behavior: Modeling and Implications for Photosynthesis and Water Use. Plant Physiology **174**, 603–613.

Vos I, Verhage A, Schuurink R, Watt L, Pieterse C, Van Wees S. 2013. Onset of herbivore-induced resistance in systemic tissue primed for jasmonate-dependent defenses is activated by abscisic acid. Frontiers in Plant Science **4**.

Vos IA, Verhage A, Watt LG, Vlaardingerbroek I, Schuurink RC, Pieterse CM, Wees SCV. 2019. Abscisic acid is essential for rewiring of jasmonic acid-dependent defenses during herbivory. , 747345.

Walker BJ, Busch FA, Driever SM, Kromdijk J, Lawson T. 2018. Survey of Tools for Measuring In Vivo Photosynthesis. In: Covshoff S, ed. Methods in Molecular Biology. Photosynthesis: Methods and Protocols. New York, NY: Springer, 3–24.

Wang M, Lee J, Choi B, Park Y, Sim H-J, Kim H, Hwang I. 2018. Physiological and Molecular Processes Associated with Long Duration of ABA Treatment. Frontiers in Plant Science **9**.

941 **Xie J, Fernandes SB, Mayfield-Jones D, Erice G, Choi M, E Lipka A, Leakey ADB**.
942 2021. Optical topometry and machine learning to rapidly phenotype stomatal patterning traits
943 for maize QTL mapping. Plant Physiology **187**, 1462–1480.

944 **Xie Z, Jiang D, Dai T, Jing Q, Cao W**. 2004. Effects of exogenous ABA and cytokinin on
945 leaf photosynthesis and grain protein accumulation in wheat ears cultured in vitro. Plant
946 Growth Regulation **44**, 25–32.

947 **Yoon D-K, Ishiyama K, Suganami M, *et al.*** 2020. Transgenic rice overproducing Rubisco
948 exhibits increased yields with improved nitrogen-use efficiency in an experimental paddy
949 field. Nature Food **1**, 134–139.

950 **Zhu S-D, Liu H, Xu Q-Y, Cao K-F, Ye Q**. 2016. Are leaves more vulnerable to cavitation
951 than branches? Functional Ecology **30**, 1740–1744.

952 **Zhu X-G, Long SP, Ort DR**. 2010. Improving Photosynthetic Efficiency for Greater Yield.
953 Annual Review of Plant Biology **61**, 235–261.

954

955 # Figure Legends

956 Figure 1. Boxplots showing differences in leaf water potential between intact and excised
957 leaves for (a) tomato, (b) barley, and (c) maize. The p-values associated with the
958 corresponding one-sample t-test are inset in each panel.

959

960 Figure 2. Boxplots showing differences in leaf ABA concentration between intact and excised
961 leaves for (a) tomato, (b) barley, and (c) maize. The p-values associated with the
962 corresponding one-sample t-test are inset in each panel.

963

964 Figure 3. Boxplots showing differences in light-saturated gas exchange between excised and
965 intact leaves in the morning (AM) and afternoon (PM) for tomato (a-d), barley (e-h), and maize
966 (i-l). Net photosynthesis (A_N), stomatal conductance (g_s), the concentration of intracellular
967 CO_2 (c_i), and intrinsic water use efficiency (*iWUE*) are shown. The p-values associated with the
968 corresponding two-way analysis of variance (ANOVA) are inset in each panel.

969

970 Figure 4. Differences in photosynthetic capacities modelled via photosynthesis-CO_2 response
971 measurements between intact and excised leaves. (a-b) The response of photosynthesis (A_N)
972 to increasing intracellular CO2 concentration (c_i) in the (a) AM and (b) PM for tomato. The
973 solid line represents the mean fit of the FvCB model and the shaded area represents the

974 standard error of the mean. (c) The maximum rate of Rubisco carboxylation (V_{cmax}) for tomato
975 in the AM and PM. (d) The maximum rate of electron transport for RuBP regeneration (J_{max})
976 for tomato in the AM and PM. (e-f) The response of A_N to increasing c_i in the (e) AM and (f)
977 PM for barley. The solid line represents the mean fit of the FvCB model and the shaded area
978 represents the standard error of the mean. (g) V_{cmax} for barley in the AM and PM. (h) J_{max} for
979 barley in the AM and PM. (i-j) The response of A_N to increasing c_i in the (i) AM and (j) PM for
980 maize. The solid line represents the mean fit of a four-parameter non-rectangular hyperbola
981 and the shaded area represents the standard error of the mean. (k) The maximum rate of
982 carboxylation by PEPc (V_{pmax}) for maize in the AM and PM. (l) The maximum rate of
983 photosynthesis (V_{max}) for maize in the AM and PM.
984
985 Figure 5. The effect of leaf excision on hyperspectral reflectance in the morning (AM) and
986 afternoon (PM) for tomato, barley, and maize. (a) AM tomato. (b) PM tomato. (c) AM barley.
987 (d) PM barley. (e) AM maize. (f) PM maize. Each panel shows the -$\log_{10}$ transformed p-value
988 from a one-way analysis of variance (ANOVA) comparing reflectance of intact and excised
989 leaves at each incremental wavelength from 350-2500nm. The dashed red lines indicate a
990 Bonferroni significance threshold ($\alpha = 0.05$).
991
992 Figure 6. Boxplots showing variation in chlorophyll fluorescence-associated traits between
993 excised and intact leaves measured in a closed chlorophyll fluorescence system. (a) Maximum
994 efficiency of photosystem II (F_v/F_m) in tomato. (b) The rate of induction of non-photochemical
995 quenching (NPQ) in tomato. (c) The rate of relaxation of NPQ in tomato. (d) Maximum NPQ
996 in tomato. (e) F_v/F_m in barley. (f) The rate of induction of NPQ in barley. (g) The rate of
997 relaxation of NPQ in barley. (h) Maximum NPQ in barley. (i) F_v/F_m in maize. (j) The rate of
998 induction of NPQ in maize. (k) The rate of relaxation of NPQ in maize. (l) Maximum NPQ in
999 maize. The p-values associated with the corresponding one-sample t-test are inset in each
1000 panel.

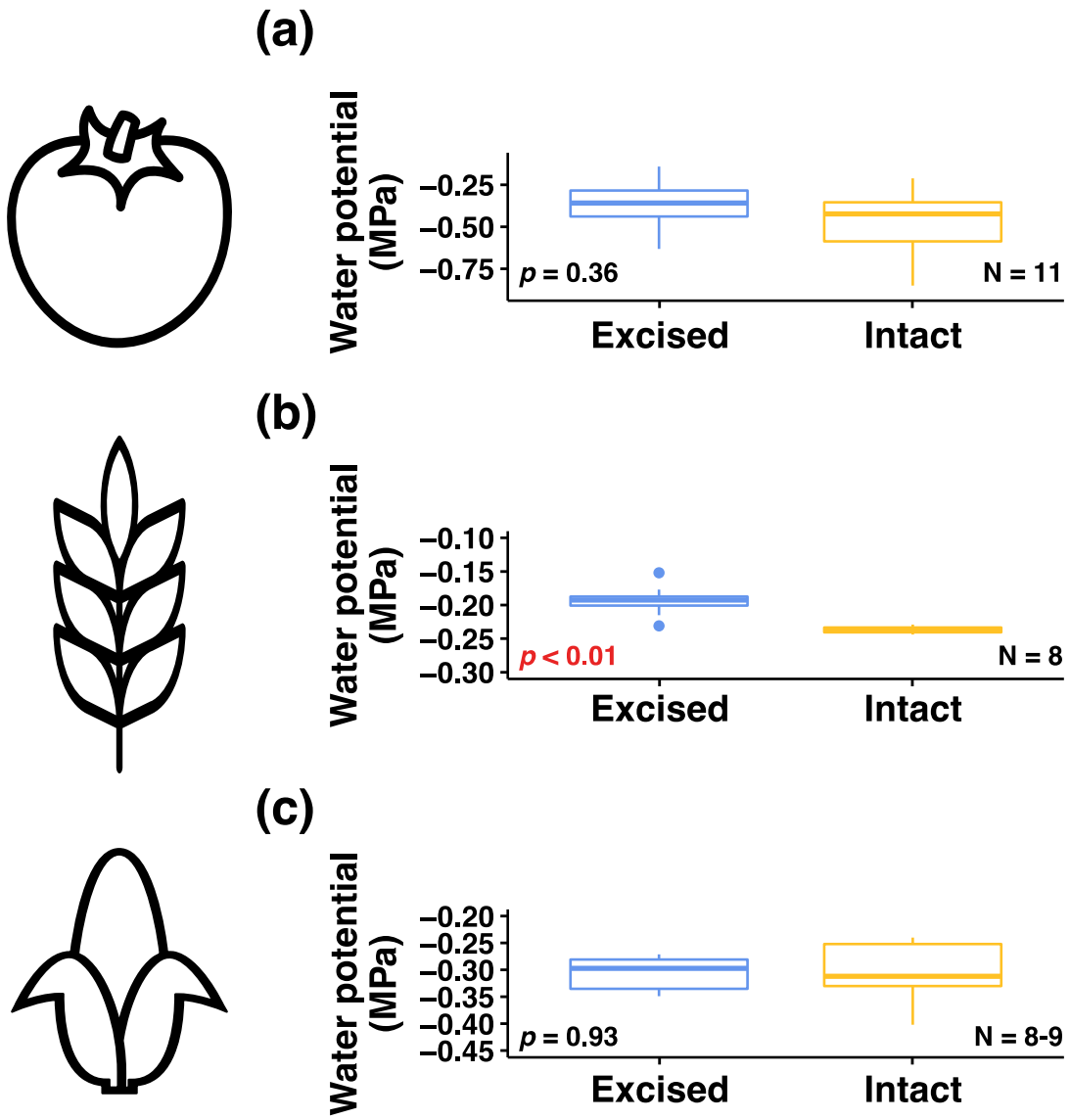

Figure 1. Boxplots showing differences in leaf water potential between intact and excised leaves for (a) tomato, (b) barley, and (c) maize. The p-values associated with the corresponding one-sample t-test are inset in each panel.

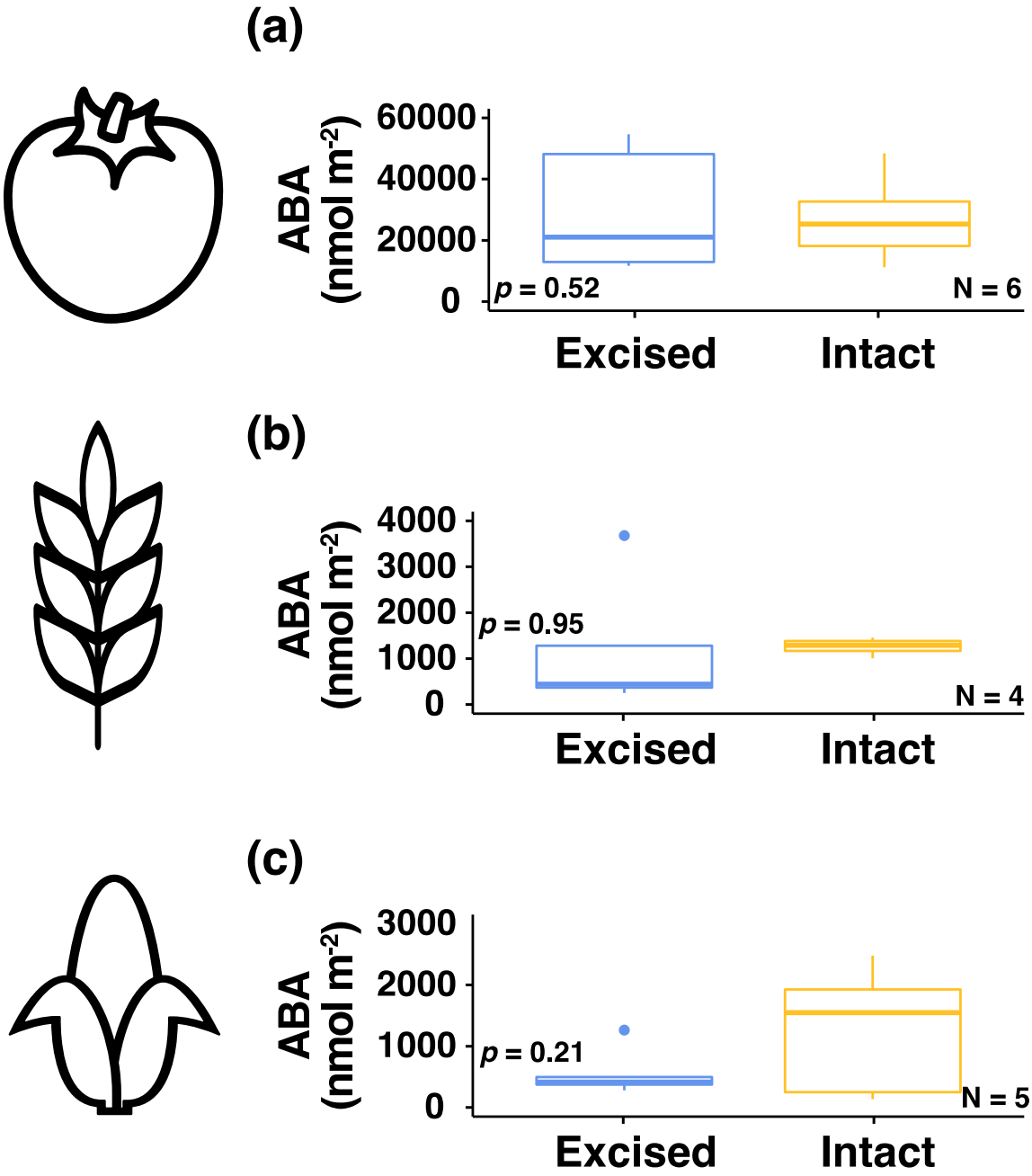

Figure 2. Boxplots showing differences in leaf ABA concentration between intact and excised leaves for (a) tomato, (b) barley, and (c) maize. The p-values associated with the corresponding one-sample t-test are inset in each panel.

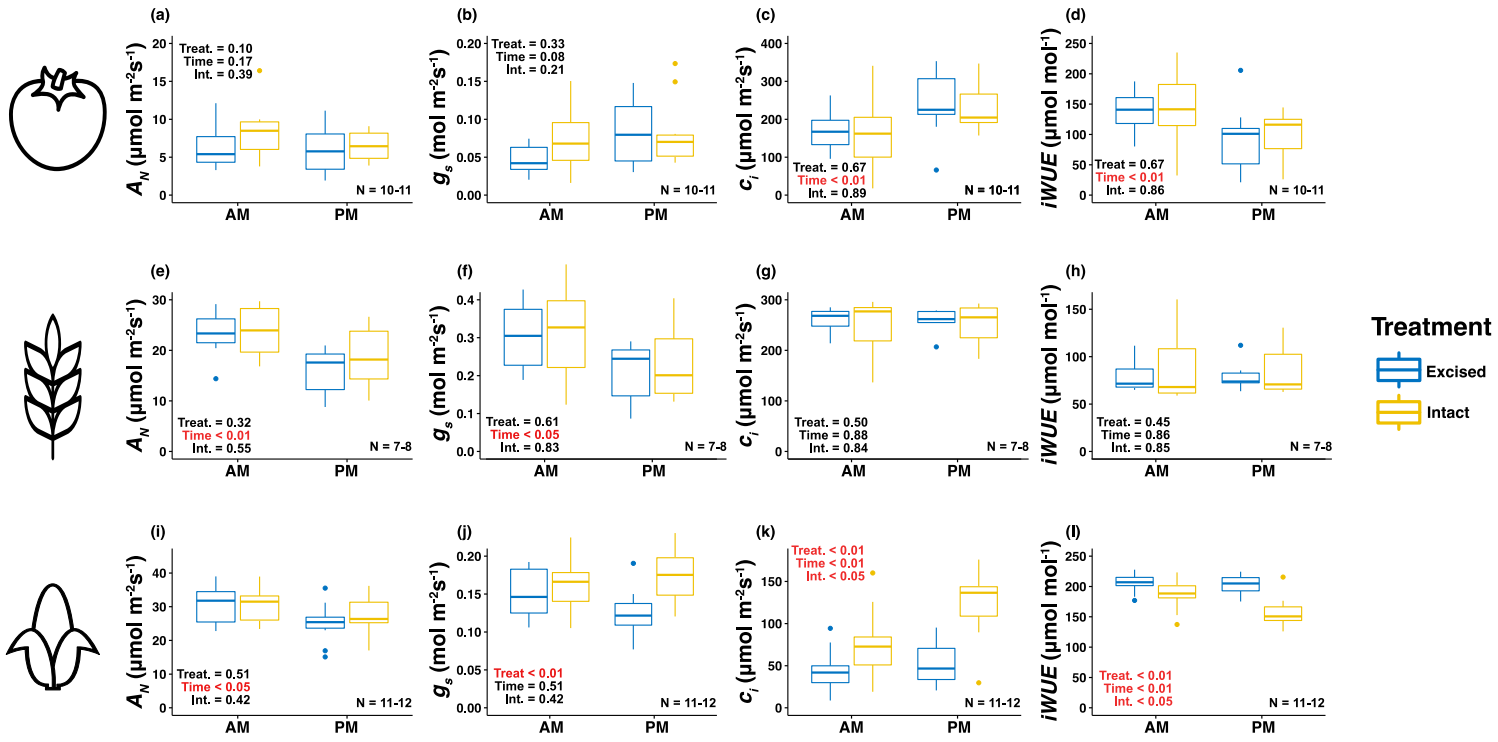

Figure 3. Boxplots showing differences in light-saturated gas exchange between excised and intact leaves in the morning (AM) and afternoon (PM) for tomato (a-d), barley (e-h), and maize (i-l). Net photosynthesis (A_N), stomatal conductance (g_s), the concentration of intracellular CO_2 (c_i), and intrinsic water use efficiency (*iWUE*) are shown. The p-values associated with the corresponding two-way analysis of variance (ANOVA) are inset in each panel.

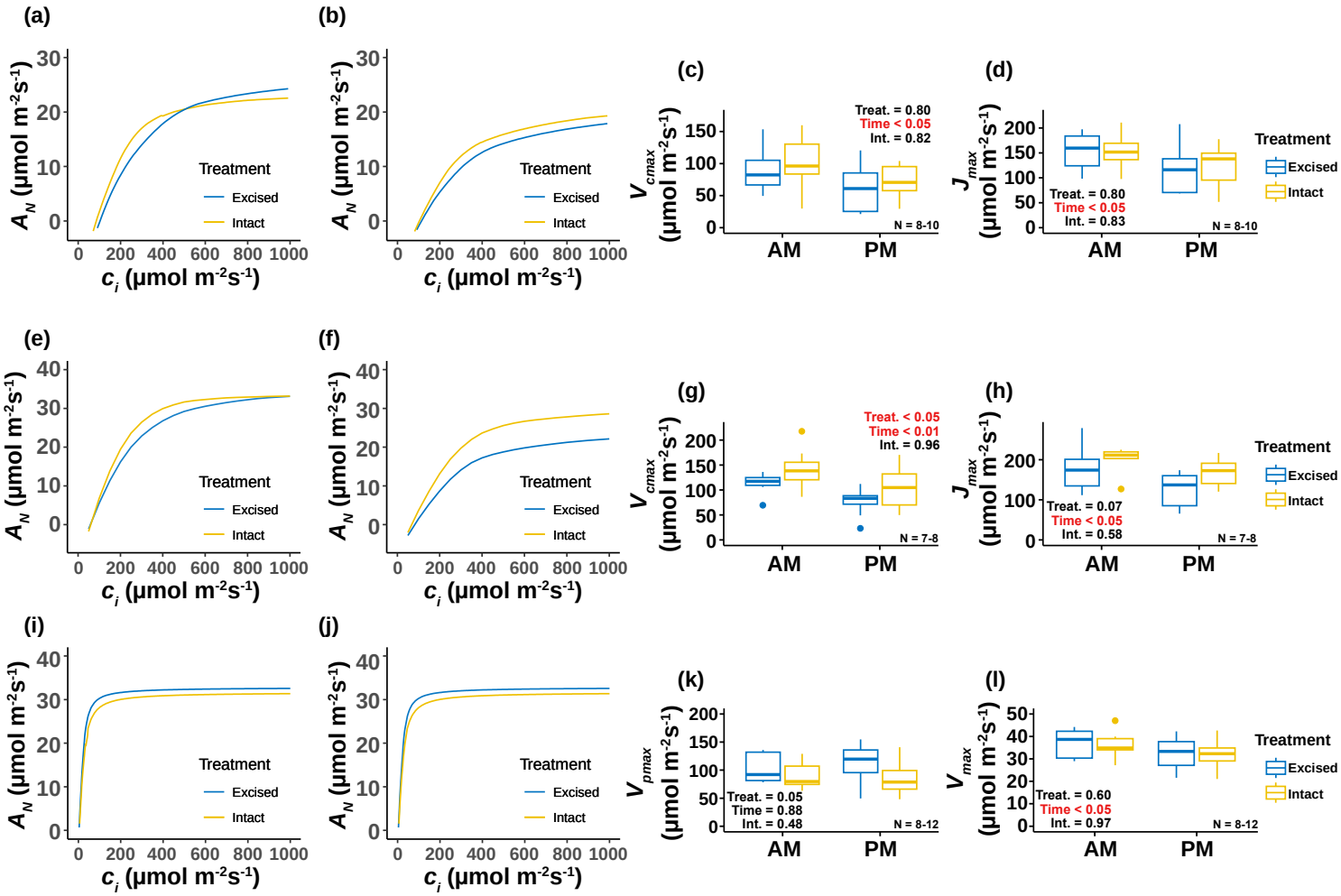

Figure 4. Differences in photosynthetic capacities modelled via photosynthesis-CO_2 response measurements between intact and excised leaves. (a-b) The response of photosynthesis (A_N) to increasing intracellular CO2 concentration (c_i) in the (a) AM and (b) PM for tomato. The solid line represents the mean fit of the FvCB model and the shaded area represents the standard error of the mean. (c) The maximum rate of Rubisco carboxylation (V_{cmax}) for tomato in the AM and PM. (d) The maximum rate of electron transport for RuBP regeneration (J_{max}) for tomato in the AM and PM. (e-f) The response of A_N to increasing c_i in the (e) AM and (f) PM for barley. The solid line represents the mean fit of the FvCB model and the shaded area represents the standard error of the mean. (g) V_{cmax} for barley in the AM and PM. (h) J_{max} for barley in the AM and PM. (i-j) The response of A_N to increasing c_i in the (i) AM and (j) PM for maize. The solid line represents the mean fit of a four-parameter non-rectangular hyperbola and the shaded area represents the standard error of the mean. (k) The maximum rate of

carboxylation by PEPc (V_{pmax}) for maize in the AM and PM. (l) The maximum rate of photosynthesis (V_{max}) for maize in the AM and PM.

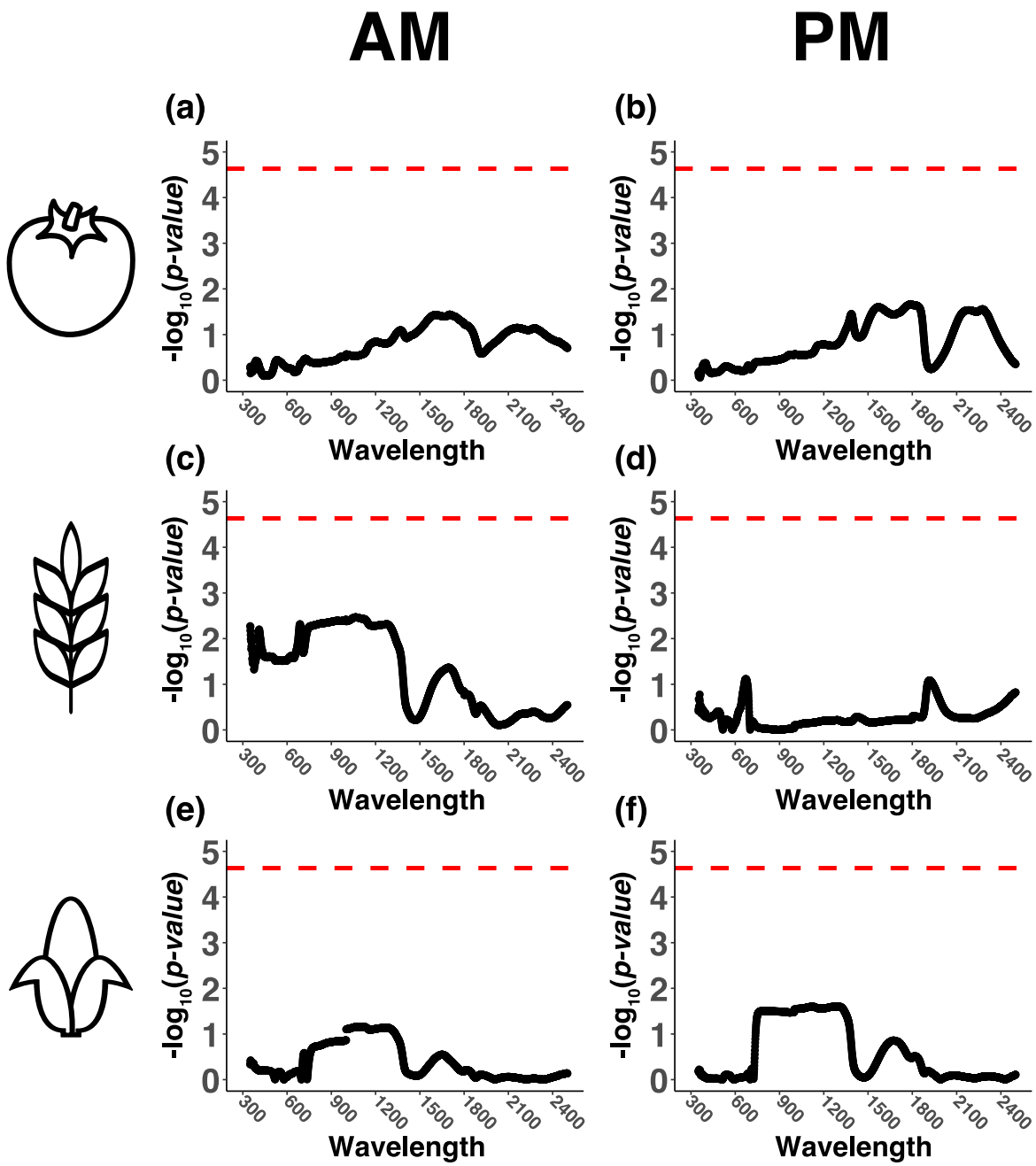

Figure 5. The effect of leaf excision on hyperspectral reflectance in the morning (AM) and afternoon (PM) for tomato, barley, and maize. (a) AM tomato. (b) PM tomato. (c) AM barley. (d) PM barley. (e) AM maize. (f) PM maize. Each panel shows the $-\log_{10}$ transformed p-value from a one-way analysis of variance (ANOVA) comparing reflectance of intact and excised leaves at each incremental wavelength from 350-2500nm. The dashed red lines indicate a Bonferroni significance threshold ($\alpha = 0.05$).

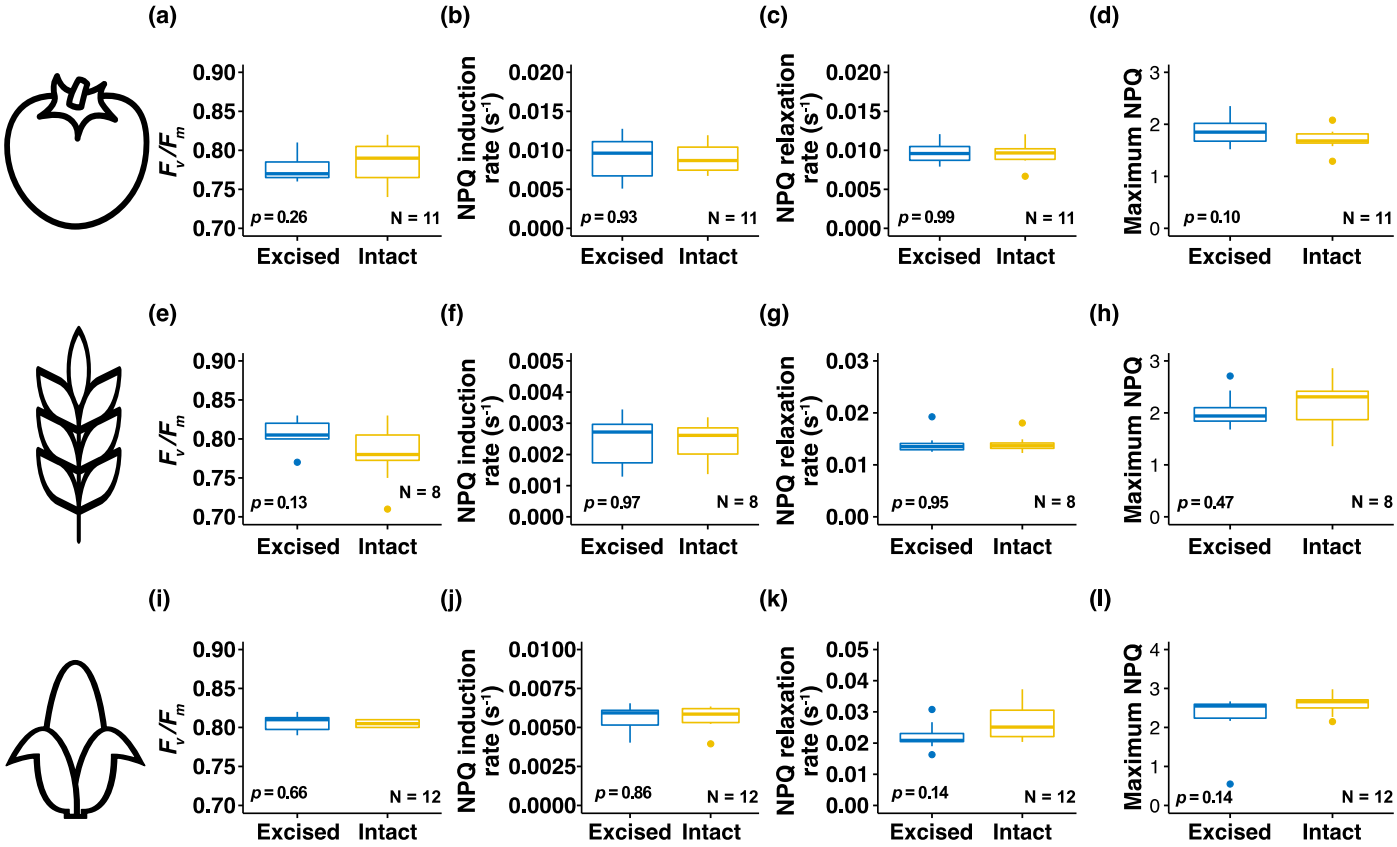

Figure 6. Boxplots showing variation in chlorophyll fluorescence-associated traits between excised and intact leaves measured in a closed chlorophyll fluorescence system. (a) Maximum efficiency of photosystem II (F_v/F_m) in tomato. (b) The rate of induction of non-photochemical quenching (NPQ) in tomato. (c) The rate of relaxation of NPQ in tomato. (d) Maximum NPQ in tomato. (e) F_v/F_m in barley. (f) The rate of induction of NPQ in barley. (g) The rate of relaxation of NPQ in barley. (h) Maximum NPQ in barley. (i) F_v/F_m in maize. (j) The rate of induction of NPQ in maize. (k) The rate of relaxation of NPQ in maize. (l) Maximum NPQ in maize. The p-values associated with the corresponding one-sample t-test are inset in each panel.